Enhanced Subband Index Carrierless Amplitude and Phase Modulation in Visible Light Communications

Enhanced Subband Index Carrierless Amplitude and Phase Modulation in Visible Light Communications

Kabiru O. Akande, *Student Member, IEEE* and Wasiu O. Popoola, *Senior Member, IEEE*
School of Engineering, Institute for Digital Communications, LiFi Research and Development Centre,
The University of Edinburgh, Edinburgh, UK
{K.Akande,W.Popoola}@ed.ac.uk

***Abstract*—An enhanced subband index carrierless amplitude and phase modulation (eSI-CAP) scheme is developed to improve the spectral efficiency of the multiband CAP (m-CAP) in visible light communication (VLC) systems. Using indexing technique and a dual distinguishable constellations, the eSI-CAP carries information bits by modulating symbols on the subbands of m-CAP. It also encodes additional information bits on the selection of the subband indices that is modulated with the dual constellation symbols. The performance advantage of eSI-CAP is demonstrated through theoretical analysis, computer simulations and VLC experimental validations. In addition, a novel maximum likelihood detector is developed for eSI-CAP with the same order of complexity as the conventional m-CAP detector. On comparison with m-CAP, eSI-CAP requires lower signal-to-noise ratio (SNR) per bit (γ_b) to reach a fixed data rate (R_b). Alternatively, when the γ_b is fixed, it achieves a higher R_b for a target BER. The results show that eSI-CAP is very attractive for VLC systems due to its flexible configuration and its improvement of the power efficiency of the conventional m-CAP modulation scheme.**

***Index Terms*—Multi-band carrierless amplitude and phase modulation (m-CAP), visible light communication (VLC), index modulation (IM), dual-mode constellation (DM).**

I. Introduction

Carrierless amplitude and phase modulation (CAP) is one of the spectrally efficient modulation techniques, along with pulse amplitude modulation (PAM) and orthogonal frequency division multiplexing (OFDM), that are employed for improving the achievable throughput in VLC systems [1]. High data rates in the range of Gb/s have been demonstrated for VLC links using the CAP technique [2].

The main attraction for CAP is its simple transceiver [1]. Early work on CAP have mainly focussed on the design and implementation of equalization techniques to improve its performance [2–4]. Recently, new contributions have taken advantage of the available groups of LEDs in VLC to implement multiple-input multiple-output (MIMO) techniques for CAP [5]. Using multiple LEDs, each with a 4 MHz 3 dB bandwidth, a MIMO CAP technique is demonstrated to achieve a data rate of 249 Mb/s at a BER of 3.2×10^{-3} in [6]. Similarly, spatial modulation techniques which carry additional information on the indices of LEDs have also been implemented to increase the achievable throughput of the conventional CAP in [7]. Furthermore, subband-indexed CAP (SI-CAP) has been proposed in [8] to improve the spectral efficiency of the multiple band version of CAP (m-CAP). However, to maintain the spectral efficiency improvement, the proposed SI-CAP requires increasing number of subbands as the modulation order increases. This requirement increases the complexity of the resulting system.

In this paper, an enhanced SI-CAP (eSI-CAP) that addresses the complexity challenge of the SI-CAP with further increase in the spectral efficiency of m-CAP is presented. Similar to m-CAP, the proposed eSI-CAP uses all its subbands for carrying data. To improve the spectral efficiency, additional information bits are encoded on the indices of these subbands.

In order to achieve the spectral efficiency improvement, eSI-CAP utilizes dual distinguishable constellations to modulate its subbands. This is in contrast to the conventional m-CAP which modulates its subbands with symbols drawn from a single constellation. The dual constellations, $\mathcal{M}_\mathrm{A}$ and $\mathcal{M}_\mathrm{B}$, are such that $\mathcal{M}_\mathrm{A} \cap \mathcal{M}_\mathrm{B} = \emptyset$ and $\mathcal{M}_\mathrm{A} \cup \mathcal{M}_\mathrm{B} = \mathcal{M}$, where $\mathcal{M}$ is the union or combination of constellations $\mathcal{M}_\mathrm{A}$ and $\mathcal{M}_\mathrm{B}$ [9, 10]. Since $\mathcal{M}_\mathrm{A}$ and $\mathcal{M}_\mathrm{B}$ are non-overlapping constellations, this makes it possible to encode additional data bits on the positions/indices of the subbands on which the constellations are modulated. Hence, eSI-CAP is able to improve the spectral efficiency of the conventional m-CAP. In this paper, the performance gain of eSI-CAP is demonstrated through theoretical analysis, computer simulations and experimental validations.

Related work include the presentation of the dual-constellation principle with OFDM in [9]. Our earlier work also showed the experimental demonstration of the dual-constellation with m-CAP in a short range optical fibre system [11]. The eSI-CAP technique is being extended to improve m-CAP performance in VLC systems in this work with the following contributions: 1.) An enhanced subband index technique is developed for m-CAP along with the derivation of its BER performance and optimum power-efficient configuration in VLC system; 2.) A novel low-complexity detector is developed for the eSI-CAP; 3.) proof-of-concept experimental demonstrations that validate the performance advantage of eSI-CAP are carried out for a VLC system. The rest of the paper is organized as follows: the model description of the proposed eSI-CAP is presented in Section II while its performance analysis and detection schemes are developed in Section III. The simulation results and experimental validations are respectively detailed in Section IV and V while Section VI concludes the paper.

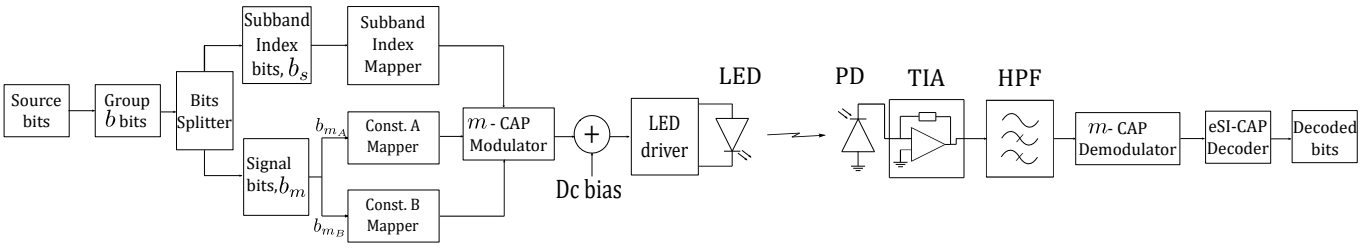

Fig. 1. The schematic block diagram of the proposed eSI-CAP transceiver for VLC link.

II. Sytem Model Description of eSI-CAP

A. Brief Description of m-CAP

The stream of information bits to be transmitted on each of the N subbands of m-CAP are first mapped to an M-QAM constellation symbols. The mapped symbols are then upsampled to match the system sampling rate and further separated into real and imaginary parts. The separated parts are respectively passed through the real and imaginary transmit filters $p(t)$ and $\bar{p}(t)$ whose outputs form independent streams. The $p(t)$ and $\bar{p}(t)$ for the nth subband are realised as follows:

$$p_n(t) = g(t)\cos(2\pi f_{c,n} t) \tag{1}$$

and

$$\bar{p}_n(t) = g(t)\sin(2\pi f_{c,n} t) \tag{2}$$

where $g(t)$ is the root raised cosine filter (RRCF) and $f_{c,n}$ is the center frequency of the nth subband given as:

$$f_{c,n} = (2n-1)f_c. \tag{3}$$

The $\{f_{c,n}\}$ are selected such that there is orthogonality between the subbands of m-CAP. The outputs of the filters, which are real, are added together with a DC-bias to ensure non-negativity. The signal is then used to modulate the intensity of the optical source and thereafter sent over the VLC channel.

The received intensity is directly detected by an optical receiver, amplified and converted to a voltage using a trans-impedance amplifier (TIA). The output of the TIA is then passed through a high pass filter (HPF) to remove the DC bias before the signal is demodulated using a conjugated, time-reversed version of the transmit filters. Thereafter, the match-filtered signal is decoded and mapped into bits.

B. Description of eSI-CAP

The proposed eSI-CAP achieves a higher spectral efficiency than the conventional m-CAP by modulating information bits on its multiple subbands as well as encoding additional bits on the index of those subbands. The block diagram of eSI-CAP model is shown in Fig. 1 for a VLC link. The stream of bits to be transmitted are grouped in blocks of b bits. Each block of b bits is further divided into the subband index bits, b_s and signal bits, b_m. The b_s bits are used to select the indices of the N_a subbands, referred to as activated subbands, that carry symbols from constellation A ($\mathcal{M}_A$). Unlike the conventional index modulation which nulls the remaining, $N_b = N - N_a$, unactivated subbands, the eSI-CAP modulates them with symbols drawn from constellation B ($\mathcal{M}_B$). Thus, $b_m = N_a \log_2(M_A) + N_b \log_2(M_B)$ where $M_A = |\mathcal{M}_A|$ and $M_B = |\mathcal{M}_B|$. Using the m-CAP modulator, the outputs of mappers A and B are modulated onto their corresponding subbands, as determined by b_s bits. At the receiver, the incoming eSI-CAP signal is first passed through an m-CAP demodulator to recover the symbols on each subband and then through an eSI-CAP decoder to recover both the index and signal bits.

TABLE I
MAPPING PROCESS FOR THE PROPOSED eSI-CAP WITH $N = 4$, $N_a = 2$ AND $M = 4$

b_s bits	$\mathcal{S} = [\mathcal{S}_A; \mathcal{S}_B]$	$\log_2(M)$ bits	$\mathcal{M}_A$	$\mathcal{M}_B$
00	[1, 2; 3, 4]	00	$+1 + j$	$+(1 + \sqrt{3})$
01	[1, 3; 2, 4]	01	$-1 + j$	$+j(1 + \sqrt{3})$
10	[1, 4; 2, 3]	10	$-1 - j$	$-(1 + \sqrt{3})$
11	[2, 3; 1, 4]	11	$+1 - j$	$-j(1 + \sqrt{3})$

The BER performance of eSI-CAP is dependent on the design of its constellations $\mathcal{M}_A$ and $\mathcal{M}_B$. To achieve a good BER performance, the minimum Euclidean distance (MED) between the dual constellation should be similar to the separation of symbols in each constituent constellation [12]. One way to achieve this is to jointly design an $(M_A + M_B)$-point constellation and then separate it into the individual constituents. As an example, Fig. 2 shows the optimum $(M_A + M_B)$-point constellation for the case of $M_A = M_B = 4$ [13]. The constellation points are given in Table I, where the inner and outer points have been allocated to $\mathcal{M}_A$ and $\mathcal{M}_B$, respectively. In comparison to its corresponding regular QAM constellation, the constellation in Fig. 2 has higher MED under a unit average power constraint which results in lower BER performance. Thus, it is adopted in this work. For other values of M_A and M_B, candidate constellations are reported in [12–14].

An example of the mapping process for the proposed eSI-CAP is illustrated as follows: consider a total number of subbands $N = 4$; active subbands $N_a = 2$ and $M_A = M_B = 4$, then there are ${}^{N}C_{N_a}$ possible ways of selecting the N_a active subbands. However, only $N_u = 2^{\lfloor \log_2({}^{N}C_{N_a}) \rfloor}$ of the possible combinations can be used to encode data bits. Thus, $N_u = 4$ and $b_s = \log_2(N_u)$. The set of selected subband indices is represented as $\mathcal{S} = \{S_{n_u}\}_{n_u=1}^{N_u}$ as shown in Table I. As an

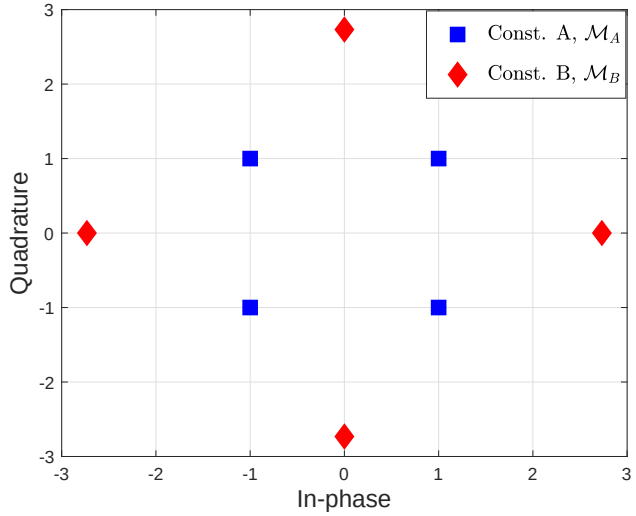

Fig. 2. The constellation symbols of eSI-CAP showing the dual distinguishable constellation mode $\mathcal{M}_{\mathrm{A}}$ and $\mathcal{M}_{\mathrm{B}}$ [9].

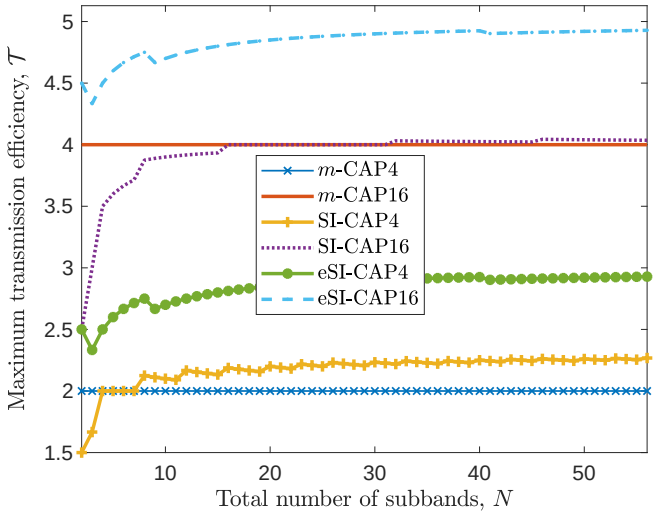

Fig. 3. The comparison of the maximum possible transmission efficiency of eSI-CAP, SI-CAP and m-CAP for a given N and M.

illustration, if bits b = '1101100111' is to be transmitted, the first b_{s} bits, '11', is encoded in the $S_{n_{\mathrm{u}}}$ selection which is $S_4 = [2, 3; 1, 4]$ in this case. This means that subbands 2 and 3 will be modulated with symbols drawn from $\mathcal{M}_{\mathrm{A}}$ while subbands 1 and 4 will be modulated with symbols drawn from $\mathcal{M}_{\mathrm{B}}$. Still using Table I, the next $N_{\mathrm{a}}\log_2(M_{\mathrm{A}})$ bits, '0110', are mapped to $\mathcal{M}_{\mathrm{A}}$ symbols $-1+j$ and $-1-j$ while the last $N_{\mathrm{b}}\log_2(M_{\mathrm{B}})$ bits, '0111′, are mapped to $\mathcal{M}_{\mathrm{B}}$ symbols $+j(1+\sqrt{3})$ and $-j(1+\sqrt{3})$. Therefore, the eSI-CAP signal vector that is sent to the m-CAP demodulator is:

$$\mathbf{x} = \begin{bmatrix} +j(1+\sqrt{3}) & -1+j & -1-j & -j(1+\sqrt{3}) \end{bmatrix}^T. \quad (4)$$

The eSI-CAP configuration can be compactly denoted by $\Omega = \left\langle {N \atop N_{\mathrm{a}}} \right\rangle_M^{\mathcal{T}}$, where M stands for the constellation size which is the same for both $\mathcal{M}_{\mathrm{A}}$ and $\mathcal{M}_{\mathrm{B}}$ and $\mathcal{T}$ represents the transmission efficiency in bits per channel use (bpcu). The $\mathcal{T}$ metric is obtained by dividing the total number of transmitted bits by the total number of subbands.

III. Performance Analysis and Detection Schemes for eSI-CAP

The BER performance analysis of the eSI-CAP model is derived based on the maximum likelihood detection scheme (MLD). Due to the high complexity of the MLD, two other low-complexity schemes that achieve similar performance as the MLD are also reported.

A. Transmission efficiency

The transmission efficiency, $\mathcal{T}$, for the eSI-CAP is expressed as:

$$\mathcal{T}_{\text{eSI-CAP}} = \frac{b_{\mathrm{s}} + b_{\mathrm{m}}}{N} \quad (5)$$

$$= \frac{\lfloor \log_2 \left({}^{N}C_{N_{\mathrm{a}}} \right) \rfloor + N_{\mathrm{a}}\log_2(M_{\mathrm{A}}) + N_{\mathrm{b}}\log_2(M_{\mathrm{B}})}{N}. \quad (6)$$

For SI-CAP that uses only the index modulation technique without the dual constellation, the $N_{\mathrm{b}}\log_2(M_{\mathrm{B}})$ term in (6) is set to zero as no data is transmitted on the 'inactive' subbands [8]. Hence,

$$\mathcal{T}_{\text{SI-CAP}} = \frac{\lfloor \log_2 \left({}^{N}C_{N_{\mathrm{a}}} \right) \rfloor + N_{\mathrm{a}}\log_2(M)}{N}. \quad (7)$$

The $\mathcal{T}_{m\text{-CAP}}$ on the other hand can not exceed $\log_2(M)$ since it is independent of N. The maximum transmission efficiency that can be obtained by eSI-CAP, SI-CAP and m-CAP for $M = 4$ and 16 are compared in Fig. 3 for a given N. The figure shows clearly that the transmission efficiency of eSI-CAP exceeds that of m-CAP and SI-CAP for the configurations considered.

B. Power efficiency

The average power allocated per subband with the conventional m-CAP without power loading is P_t/N, where P_t is the total transmitted power. However, the average power per subband for the proposed eSI-CAP is $\zeta P_{\mathrm{t}}/N$, where:

$$\zeta = \frac{N}{N_{\mathrm{a}}E_{\mathrm{a}} + N_{\mathrm{b}}E_{\mathrm{b}}}. \quad (8)$$

Both E_{a} and E_{b} respectively refer to the average energy of $\mathcal{M}_A$ and $\mathcal{M}_B$ with $\mathcal{M}$ normalized to unit average energy. Since $E_{\mathrm{b}} > E_{\mathrm{a}}$, (8) shows that the configuration with higher N_{a} is the most power efficient for a fixed N and $\mathcal{T}$. Intuitively, this will be the configuration with most symbols drawn from the lower-energy constellation $\mathcal{M}_A$. For example, if $N = 4$ then $N_{\mathrm{a}} = 1, 2$ and 3 all result in $\mathcal{T} = 2.5$ bpcu. However, using the constellation depicted in Fig. 2, the average transmitted power required for the case of $N_{\mathrm{a}} = 1, 2$ and 3 are 1.29 W, 1 W and 0.71 W, respectively. Although the three configurations have the same $\mathcal{T}$, the configuration with $N_{\mathrm{a}} = 3$ is the most power efficient. Hence, it can be stated that for a fixed transmission efficiency, increasing the active number of subbands results in a configuration that requires less transmitted power. The insight provided by (8) enables the use of optimum

$$BER_{\text{eSI-CAP}} \leq \frac{1}{K\log_2(K)} \sum_{k=1}^{K} \sum_{\tilde{k}=1}^{K} \mathcal{N}_H(b_k, \tilde{b}_k) Q\left(\sqrt{\frac{(\zeta \mathcal{K} \beta \Re)^2}{2N_0} \left\| h\left(\mathbf{x}_k - \tilde{\mathbf{x}}_k\right)\right\|^2}\right). \tag{16}$$

configuration to obtain the best performance for eSI-CAP. This will later be confirmed with simulation results and validated through an experimental demonstration.

C. eSI-CAP with Maximum Likelihood Detector (MLD)

Considering a line-of-sight (LOS) channel with gain h, the eSI-CAP signal obtained at the output of the m-CAP demodulator can be expressed as:

$$\mathbf{y} = \zeta \mathcal{K} \beta \Re h \mathbf{x}_k + \mathbf{w} \tag{9}$$

where y_n, $x_{k,n}$ and w_n represent the nth subband component of $N \times 1$ vectors $\mathbf{y}$, $\mathbf{x}_k$ and $\mathbf{w}$, respectively. $x_{k,n}$ is the transmitted symbol that is drawn from $\mathcal{M}$ as shown in (4). The responsivity of the photodetector is represented as $\Re$ while w_n is the noise component modelled as additive white Gaussian noise (AWGN) with zero mean and double-sided power spectral density $N_0/2$. Both $\mathcal{K}$ and β represent the electrical-to-optical conversion coefficient and the optical modulation index, respectively. By letting $\boldsymbol{\psi}_k = \zeta \mathcal{K} \beta \Re h \mathbf{x}_k$, (9) can be compactly expressed as

$$\mathbf{y} = \boldsymbol{\psi}_k + \mathbf{w}. \tag{10}$$

Since the eSI-CAP symbol $\{\mathbf{x}_k\}_{k=1}^{K}$ with $K = N_{\text{u}} M_{\text{A}}^{N_{\text{a}}} M_{\text{B}}^{N_{\text{b}}}$ is equiprobable with a probability of $1/K$, the ML criterion that maximizes the probability density function of $\mathbf{y}$ given $\boldsymbol{\psi}_k$ can be expressed as:

$$\hat{\mathbf{x}}_k = \arg\max_{k} p(\mathbf{y}, \boldsymbol{\psi}_k) \tag{11}$$

where,

$$p(\mathbf{y}, \boldsymbol{\psi}_k) = \frac{1}{(2\pi N_0)^{N/2}} \exp\left[-\frac{\|\mathbf{y} - \boldsymbol{\psi}_k\|^2}{2N_0}\right] \tag{12}$$

The ML criteria of (11) can be reduced to the minimum distance criteria as:

$$\hat{\mathbf{x}}_k = \arg\min_{k} D(\mathbf{y}, \boldsymbol{\psi}_k) \tag{13}$$

where the MED metric $D(\mathbf{y}, \boldsymbol{\psi}_m)$ is expressed as:

$$D(\mathbf{y}, \boldsymbol{\psi}_k) = \|\mathbf{y} - \boldsymbol{\psi}_k\|^2 \tag{14}$$

Using the pairwise error probability (PEP), the eSI-CAP detector considers the joint detection of both the subband index combination and the transmitted symbols. The PEP for eSI-CAP is therefore defined as the probability of error for detecting $\tilde{\mathbf{x}}_k$ instead of the actual transmitted symbol $\mathbf{x}_k$ and is derived as:

$$\begin{aligned} PEP_{\text{eSI-CAP}} &= p(\mathbf{x}_k \rightarrow \tilde{\mathbf{x}}_k) \\ &= Q\left(\sqrt{\frac{(\zeta \mathcal{K} \beta \Re)^2}{2N_0} \left\| h\left(\mathbf{x}_k - \tilde{\mathbf{x}}_k\right)\right\|^2}\right). \end{aligned} \tag{15}$$

The PEP of (15) is then used to obtain an upper bound BER expression that is shown in (16). The expression is obtained by considering all the possible K combinations of the eSI-CAP symbols using the union bound technique. The $\mathcal{N}_H(b_k, \tilde{b}_k)$ is the number of bits in error when $\tilde{\mathbf{x}}_k$ is detected instead of the actual transmitted symbol $\mathbf{x}_k$.

However, the MLD computes the MED between each received symbol and all the possible $K = N_{\text{u}} M_{\text{A}}^{N_{\text{a}}} M_{\text{B}}^{N_{\text{b}}}$ symbols in order to make a decision. Thus, its computational complexity is of the order $\mathcal{O}(K)$, which grows exponentially and becomes infeasible as the constellation size and number of subbands increase. In order to address this, two other lower complexity detection schemes are presented.

D. eSI-CAP with Log Likelihood Ratio Detector (LLR)

The LLR considers the logarithm of the ratio of the a *posteriori* probabilities for each received subband symbol. It uses the fact that the subband symbol can either be drawn from $\mathcal{M}_A = \{s_{m_{\text{a}}}\}_{m_{\text{a}}=1}^{M_{\text{A}}}$ or $\mathcal{M}_B = \{s_{m_{\text{b}}}\}_{m_{\text{b}}=1}^{M_{\text{B}}}$. The formulation for the LLR can be stated as:

$$\chi_n = \ln\left(\frac{\sum_{m_{\text{a}}=1}^{M_{\text{A}}} \Pr(x_n = s_{m_{\text{a}}} | y_n)}{\sum_{m_{\text{b}}=1}^{M_{\text{B}}} \Pr(x_n = s_{m_{\text{b}}} | y_n)}\right) \tag{17}$$

where x_n and y_n respectively represent the transmitted and received symbols on the nth subband. Using Baye's theorem, (17) can be restated as:

$$\chi_n = \ln\left(\frac{\sum_{m_{\text{a}}=1}^{M_{\text{A}}} \Pr(y_n | x_n = s_{m_{\text{a}}}) \Pr(x_n = s_{m_{\text{a}}})}{\sum_{m_{\text{b}}=1}^{M_{\text{B}}} \Pr(y_n | x_n = s_{m_{\text{b}}}) \Pr(x_n = s_{m_{\text{b}}})}\right) \tag{18}$$

and given the AWGN channel, the conditional probabilities can be expressed as:

$$\Pr(y_n | x_n = s_{m_{\text{a}}}) = \frac{1}{(2\pi N_0)^{1/2}} \exp\left[-\frac{\left|y_n - s_{m_{\text{a}}} h\right|^2}{2N_0}\right] \tag{19}$$

and

$$\Pr(y_n | x_n = s_{m_{\text{b}}}) = \frac{1}{(2\pi N_0)^{1/2}} \exp\left[-\frac{\left|y_n - s_{m_{\text{b}}} h\right|^2}{2N_0}\right]. \tag{20}$$

By substituting (19) and (20) in (18) and considering the fact that $\Pr(x_n = s_{m_{\text{a}}}) = N_{\text{a}}/NM_{\text{A}}$ while $\Pr(x_n = s_{m_{\text{b}}}) = (N - N_{\text{a}})/NM_{\text{B}}$, the LLR values for each subband can be computed as follows:

$$\begin{aligned} \chi_n = \ln\left(\frac{M_{\text{B}} N_{\text{a}}}{M_{\text{A}}(N - N_{\text{a}})}\right) + \ln\left(\sum_{m_{\text{a}}=1}^{M_{\text{A}}} \exp\left[-\frac{\left|y_n - s_{m_{\text{a}}} h\right|^2}{2N_0}\right]\right) \\ - \ln\left(\sum_{m_{\text{b}}=1}^{M} \exp\left[-\frac{\left|y_n - s_{m_{\text{b}}} h\right|^2}{2N_0}\right]\right). \end{aligned} \tag{21}$$

The LLR computations of (21) is prone to computational overflow which can be avoided by employing the Jacobian logarithm [15]. The computed LLR values, $\{\chi_n\}_{n=1}^{N}$, are arranged in decreasing order and the indices of the first N_{a} entries are taken as the activated subband index combination. Using the already detected N_{a} indices, the remaining N_{b} indices that complete the detected $S_{n_{\text{u}}}$ is easily determined as shown in Table I. Thereafter, $\mathcal{M}_{\text{A}}$ and $\mathcal{M}_{\text{B}}$ decoders are employed to detect the symbols on the subbands in

accordance with the detected S_{n_u}.
Because the LLR has no knowledge of the subband index combinations that are employed, it is possible to decide on some $S_{n_u} \notin \mathcal{S}$ especially when the noise variance is high. Since this is an error event, such cases can be resolved by randomly mapping the detected combination to any of the entries in $\mathcal{S}$.

E. eSI-CAP with Low Complexity Detector (LCD)

The LLR detector of (21) requires the knowledge of noise variance and is also susceptible to computational overflow. As a result, a novel lower complexity detector is developed to address these issues. The proposed LCD employs the knowledge of $\mathcal{M}_A$ and $\mathcal{M}_B$, which is known to the receiver, to compute the MED between the received subband symbol and the constellation points. It then selects the most likely of the constellation symbols based on the computed values. The proposed LCD is therefore formulated as:

$$\lambda_n = \min_{m_a} |y_n - s_{m_a} h|^2. \tag{22}$$

After evaluating (22) for $\{y_n\}_{n=1}^{N}$, the LCD then proceeds to select the indices that correspond to the first N_a entries of $\{\lambda_n\}$ when sorted in ascending order as the active subband index combination. Using the detected active indices, the S_{n_u} is easily determined as shown in Table I. The $\mathcal{M}_A$ and $\mathcal{M}_B$ decoders are then respectively employed to determine the symbol bits carried on the detected active and inactive subbands. Similar to LLR, the LCD is also prone to detect some $S_{n_u} \notin \mathcal{S}$. In such cases, the random mapping solution is also implemented.

The complexity of LCD is of order $\mathcal{O}(NM_A)$ as its decision criteria in (22) shows that it computes the MED between each received N symbols and the M_A constellation points. Thus, its complexity is much lower than that of the MLD. A comparison of the LCD and LLR also show that the LCD has lower complexity as it only computes a part of the second term in (21). Furthermore, the LCD dispenses with the knowledge of the noise variance and is not susceptible to computational overflow. In addition, the LCD achieves similar BER performance with MLD especially at high SNR.

IV. Simulation Results and Discussions

Computer simulations are conducted to investigate the performance of the proposed eSI-CAP. For the simulations, the electrical signal-to-noise ratio (SNR) per bit is defined as $\gamma_b = \frac{(\zeta \mathcal{K} \beta \Re)^2}{\mathcal{T} N_0}$ where $\mathcal{T}$ is $\log_2(M)$ for m-CAP and it is as defined in (6) and (7) for eSI-CAP and SI-CAP, respectively.

The BER against SNR for the various configurations of eSI-CAP and comparison of its detection schemes is depicted in Fig. 4. For $N = 4$, eSI-CAP configurations using $N_a = 1, 2$ and 3 all result in the same $\mathcal{T} = 2.5$ bpcu. However, as shown in Fig. 4, the configuration with $N_a = 3$ requires an γ_b of 9.35 dB to achieve a BER of 10^{-4} compared to the cases of $N_a = 1$ and 2 which require 11.25 dB and 10.6 dB, respectively. Thus, an γ_b of ~2 dB is gained by using the optimum configuration. This confirms

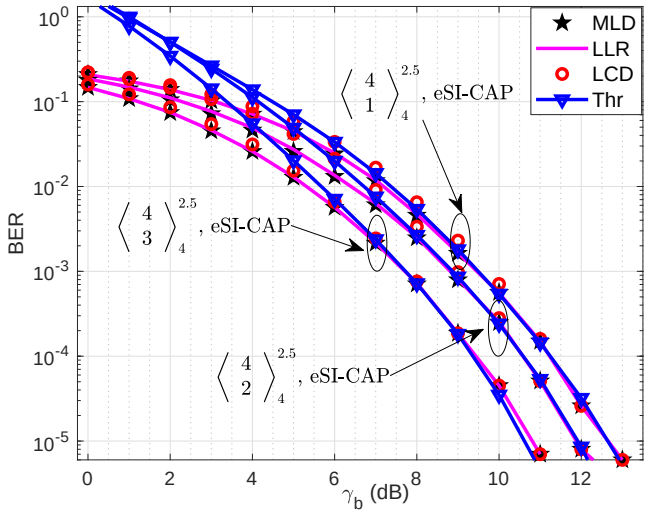

Fig. 4. A demonstration of the optimum power-efficient eSI-CAP configuration and comparison of its detection schemes showing excellent agreement with the derived theoretical analysis.

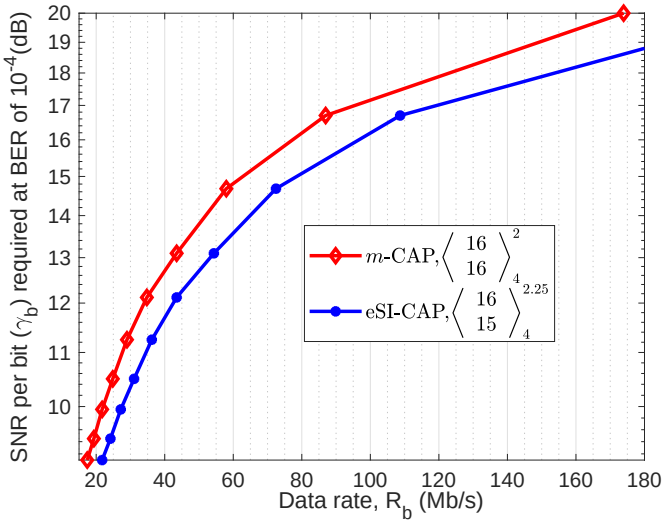

Fig. 5. The comparison of the SNR per bit (γ_b) required by eSI-CAP and m-CAP schemes to achieve BER of 10^{-4} at varying R_b in VLC channel modelled as first-order low-pass filter with a 10 MHz 3 dB cut-off frequency.

the analysis presented in Section III-B. Furthermore, the LCD achieves similar performance as the LLR and MLD especially at high SNR. Therefore, LCD is the most attractive for eSI-CAP as it has the lowest complexity, is not susceptible to computational overflow and does not require the knowledge of the noise variance. Also, the MLD analysis derived in (16) is validated and shown to match with the simulations, especially at high SNR. Finally, it can be inferred that the MLD analysis is valid for both LLR and LCD as they all achieve similar BER performances.

The γ_b required to achieve a BER of 10^{-4} at different data rates (R_b) under the effect of VLC limited bandwidth is compared for all the schemes in Figs. 5 and 6. The effect of LED bandwidth limitation is modelled as a first-order

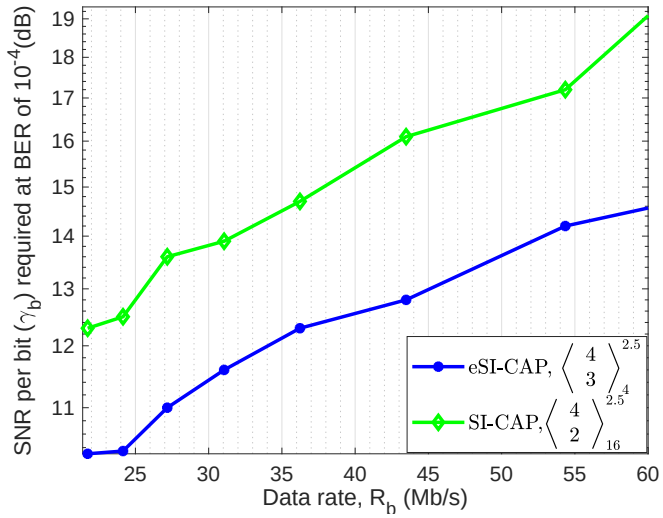

Fig. 6. The comparison of the SNR per bit (γ_b) required by eSI-CAP and SI-CAP schemes to achieve BER of 10^{-4} at varying R_b in VLC channel modelled as first-order low-pass filter with a 10 MHz 3 dB cut-off frequency.

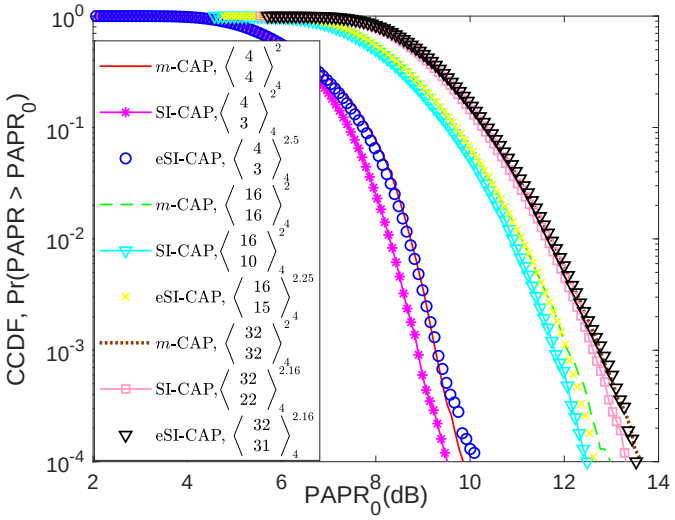

Fig. 7. The comparison of the complimentary cumulative distribution function (CCDF) of the peak-to-average power ratio (PAPR) of eSI-CAP, SI-CAP and m-CAP for $N = 4$, 16 and 32.

low-pass filter with a 3 dB cut-off frequency of 10 MHz, for illustration purposes. It is shown in both figures that eSI-CAP achieves better BER performance when compared to SI-CAP and the conventional m-CAP over the range of data rates investigated. For example, when the $R_b = 60$ Mb/s in Fig. 5, eSI-CAP requires an γ_b of 13.5 dB to achieve a BER of 10^{-4} compared to 14.8 dB required by m-CAP. Alternatively, at an γ_b of 16 dB, eSI-CAP achieves $R_b = 96.5$ Mb/s at a BER of 10^{-4} compared to $R_b = 77.5$ Mb/s achieved by m-CAP. With these comparisons, eSI-CAP is able to provide an γ_b gain of 1.3 dB at a fixed R_b or up to 19 Mb/s data rate improvement when the γ_b is fixed. Similarly, the performance of both eSI-CAP and SI-CAP have been compared in Fig. 6. Due to the fundamental difference in the two schemes, it is not possible to use similar parameters for a fair comparison. As a result, the transmission efficiency has been fixed in the comparison. It is shown that at $R_b = 60$ Mb/s in Fig. 6, eSI-CAP requires an γ_b of 14.6 dB while SI-CAP requires 19 dB. When the γ_b is fixed at 15 dB, eSI-CAP achieves $R_b = 66$ Mb/s compared to $R_b = 37.9$ Mb/s achieved by SI-CAP. Therefore, it can be concluded that at a fixed data rate, eSI-CAP achieves better power efficiency compared to other schemes. And if the power efficiency is fixed, eSI-CAP will achieve a higher data rate for the same BER performance.

The complimentary cumulative distribution function (CCDF) of the peak-to-average power ratio (PAPR) for all the schemes are compared in Fig. 7 with $N = 4, 16$ and 32. The figure shows that for small number of subbands, $N = 4$, and for any given PAPR threshold, the CCDF of SI-CAP is lower than that of both m-CAP and eSI-CAP. However, as N increases, the CCDF plots of all the three schemes have slight but insignificant differences. So, for $N > 4$, it can be concluded that implementing eSI-CAP does not result in PAPR penalty over the conventional m-CAP.

V. Experimental Validation of eSI-CAP Performance

An experimental demonstration of the eSI-CAP in VLC is carried out using a commercially available LED. Figure 8 illustrates the set-up employed for the VLC experimental demonstration. The SI-CAP and m-CAP are also experimented for comparison. The information bits, consisting of 2^{20} pseudo-random binary sequence, for eSI-CAP, SI-CAP and m-CAP are generated offline and mapped to the corresponding symbols. Thereafter, the modulated symbols are sent to an arbitrary waveform generator (AWG, Agilent 33600 series) to generate a continuous waveform. The AWG output is sent to a Bias-T where it is added with a DC bias to ensure non-negativity. A high brightness blue LED (OSRAM LDCN5M, [8]) with a -3 dB cut-off frequency of 10.8 MHz is used as the optical source while an off-the-shelf PIN photodiode (THORLABS PDA10A(-EC) with a bandwidth of 150 MHz) is employed as the receiver. Optical lenses are employed both at the transmitting and receiving end to ensure that most of the optical radiation are focussed on the receiving PD. The receiving PD output is captured in real time with an Agilent 7000B Series oscilloscope. The signal is then processed offline in order to recover the transmitted bits. The results are presented without any forward error correction codes (FEC).

The most power-efficient configuration for eSI-CAP is experimentally validated with the results shown in Fig. 9. The configuration with $N_a = 3$ achieves better BER performance over the range of modulation index, β and data rates, R_b investigated. Specifically, at $R_b = 153$ Mb/s and $\beta = 0.06$, the configuration with $N_a = 3$ achieves the lowest BER of 1.5×10^{-3} compared to 4×10^{-3} and 7×10^{-3} achieved by the configurations with $N_a = 2$ and 1,

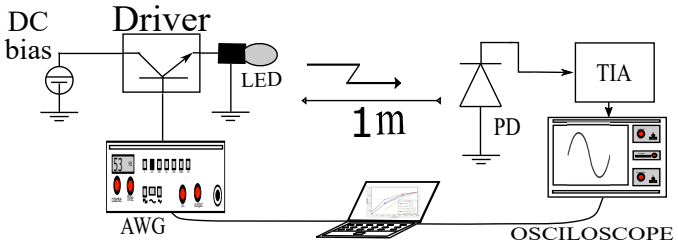

Fig. 8. Illustration of the VLC experimental demonstration set-up.

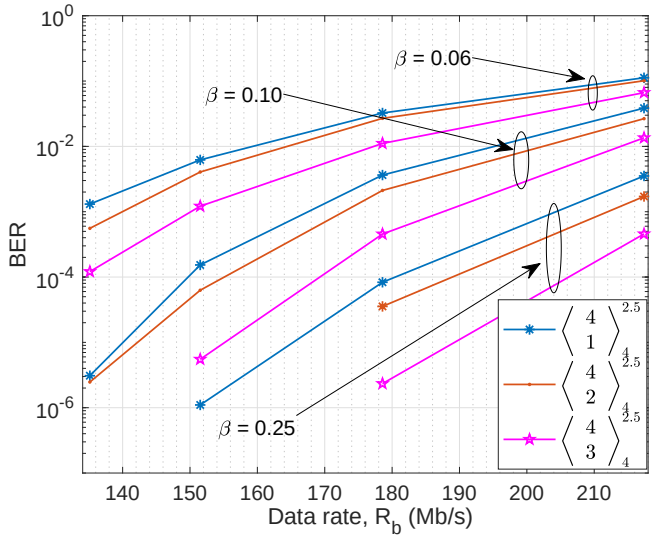

Fig. 9. Experimental validation of the optimum power-efficient configuration for eSI-CAP in a VLC link with a 3 dB bandwidth of 10.9 MHz at varying β and R_b.

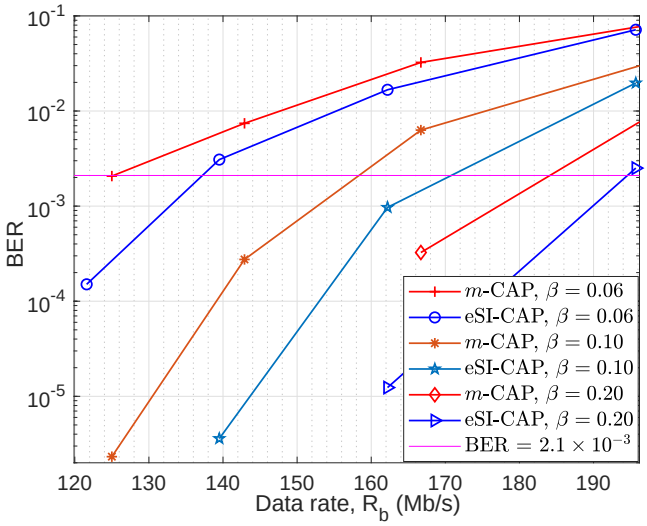

Fig. 10. Experimental validation of the superior BER performance of eSI-CAP in VLC when compared to m-CAP at varying modulation index, β and data rates, R_b using a commercially available LED with a link bandwidth of 10.9 MHz.

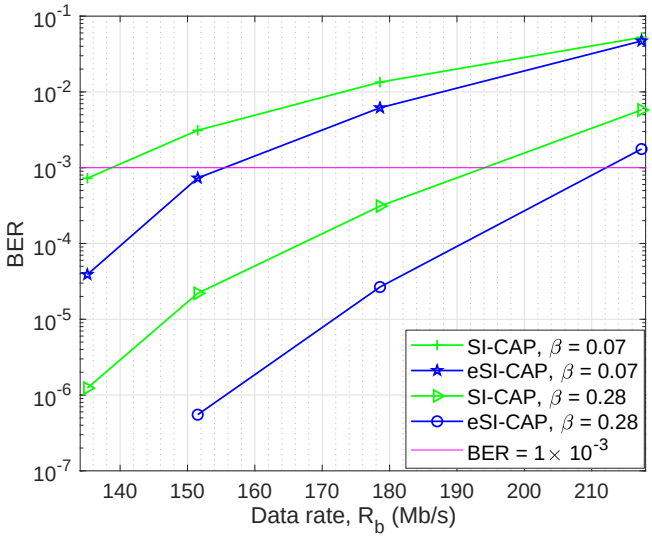

Fig. 11. Experimental validation of the superior BER performance of eSI-CAP in VLC when compared to SI-CAP at varying modulation index, β and data rates, R_b using a commercially available LED with a link bandwidth of 10.9 MHz.

respectively. Furthermore, when the BER is fixed at 1×10^{-4} and $\beta = 0.10$, the configuration with $N_a = 3$ achieves a bit rate R_b of 169 Mb/s compared to 155 Mb/s and 150 Mb/s achieved by the configurations with $N_a = 2$ and 1, respectively. At the same BER of 1×10^{-4} but higher $\beta = 0.25$, the R_b is 206 Mb/s, 189 Mb/s and 180 Mb/s respectively for $N_a = 3, 2$ and 1. It should be noted that the higher modulation index corresponds to higher SNR at the receiver, hence the improved performance. Therefore, for a fixed N and R_b, the eSI-CAP configuration with the highest N_a is the most power-efficient. This provides experimental validation for the simulation result of Fig. 4 and the analysis of section III-B.

The performances of eSI-CAP and m-CAP in the VLC experimental demonstration is presented in Fig. 10 for varying values of R_b and β. The same configurations used in Fig. 5 is adopted for the experimental validation. Considering a BER of 2.1×10^{-3} which is lower than the FEC BER limit, the eSI-CAP outperforms m-CAP for the range of R_b and β values investigated. At BER of 2.1×10^{-3} and $\beta = 0.06$, implementing eSI-CAP results in a R_b improvement of 12 Mb/s as eSI-CAP achieves R_b of 137 Mb/s compared to 125 Mb/s achieved by m-CAP. The eSI-CAP scheme maintains its advantage when the β is increased to 0.1 and 0.20 as it achieves a corresponding R_b of 171 Mb/s and 195 Mb/s compared to 159 Mb/s and 184 Mb/s achieved by m-CAP. Therefore, the eSI-CAP achieve a R_b gain of ~12 Mb/s when compared to m-CAP over the range of R_b and β values investigated in the VLC experimental demonstration.

Similarly, Fig. 11 depicts the performance comparison of eSI-CAP and SI-CAP in the VLC experimental demonstration using the same configurations adopted in Fig. 6. At a BER of 1×10^{-3} and $\beta = 0.07$, the eSI-CAP provides a data rate gain of 17.5 Mb/s as it achieves $R_b = 157$ Mb/s compared to 139.5 Mb/s achieved by SI-CAP. When the β is increased to 0.28, the eSI-CAP

TABLE II
A SUMMARY OF THE DATA RATE ACHIEVED BY eSI-CAP COMPARED TO m-CAP AND SI-CAP USING DIFFERENT MODULATION INDEX (β) AT BER OF 2.1×10^{-3} AND 1×10^{-3}, RESPECTIVELY.

Scheme \ β	0.20	0.10	0.06	0.28	0.07
	(BER = 2.1×10^{-3})			(BER = 1×10^{-3})	
$R_{b(\text{eSI-CAP})}$ (Mb/s)	195	171	137	212.6	157
$R_{b(m\text{-CAP})}$ (Mb/s)	184	159	125	–	–
$R_{b(\text{SI-CAP})}$ (Mb/s)	–	–	–	195.1	139.5

maintains its advantage as it achieves R_b of 212.6 Mb/s compared to 195.1 Mb/s achieved by SI-CAP. Thus, eSI-CAP provides a R_b gain of ∼17.5 Mb/s when compared to SI-CAP over the range of R_b and β values investigated in the VLC experimental demonstration. It can therefore be concluded, based on the simulation results that have been validated by the experimental demonstrations, that eSI-CAP is a very attractive scheme for VLC systems. A summary of the performance comparison of all the schemes is presented in Table II for added clarity.

VI. CONCLUSION

An enhanced SI-CAP (eSI-CAP) modulation scheme has been developed for VLC systems which uses subband indexing technique to improve the performance of the conventional m-CAP scheme. The eSI-CAP not only transmit information bits by modulating the subbands of the m-CAP but also carries additional bits on the selection of the subband indices using a dual distinguishable constellations. An ML detector of the same complexity order as the m-CAP detector is developed while the optimum power-efficient configuration for eSI-CAP is also derived. The developed eSI-CAP is shown through theoretical analysis, computer simulations and experimental demonstrations to result in better performance when compared to the SI-CAP and m-CAP schemes. At a fixed data rate, the eSI-CAP requires less SNR per bit to achieve a target BER thus providing higher power efficiency. Alternatively, when the SNR per bit is fixed, the eSI-CAP achieves a higher data rate for a target BER. Therefore, the eSI-CAP represents an attractive scheme for VLC systems as it provides flexible design along with improving the spectral/power efficiency of the conventional m-CAP modulation scheme.

REFERENCES

[1] G. Stepniak, L. Maksymiuk, and J. Siuzdak, "Experimental comparison of PAM, CAP, and DMT modulations in phosphorescent white LED transmission link," *IEEE Photonics Journal*, vol. 7, no. 3, pp. 1–8, June 2015.

[2] Y. Wang *et al.*, "8-Gb/s RGBY LED-based WDM VLC system employing high-order CAP modulation and hybrid post equalizer," *IEEE Photonics Journal*, vol. 7, no. 6, pp. 1–7, Dec 2015.

[3] Y. Wang, L. Tao, Y. Wang, and N. Chi, "High speed WDM VLC system based on multi-band CAP-64 with weighted pre-equalization and modified CMMA based post-equalization," *IEEE Communications Letters*, vol. 18, no. 10, pp. 1719–1722, Oct 2014.

[4] P. A. Haigh *et al.*, "A multi-CAP visible-light communications system with 4.85-b/s/Hz spectral efficiency," *IEEE Journal on Selected Areas in Communications*, vol. 33, no. 9, pp. 1771–1779, Sept 2015.

[5] K. O. Akande and W. O. Popoola, "MIMO techniques for carrierless amplitude and phase modulation in visible light communication," *IEEE Communications Letters*, vol. 22, no. 5, pp. 974–977, May 2018.

[6] K. Werfli *et al.*, "Experimental demonstration of high-speed 4×4 imaging multi-CAP MIMO visible light communications," *Journal of Lightwave Technology*, vol. 36, no. 10, pp. 1944–1951, May 2018.

[7] K. O. Akande and W. O. Popoola, "Spatial carrierless amplitude and phase modulation technique for visible light communication systems," *IEEE Systems Journal*, pp. 1–10, 2019.

[8] K. O. Akande and W. O. Popoola, "Subband index carrierless amplitude and phase modulation for optical communications," *Journal of Lightwave Technology*, vol. 36, no. 18, pp. 4190–4197, Sep. 2018.

[9] T. Mao, Z. Wang, Q. Wang, S. Chen, and L. Hanzo, "Dual-mode index modulation aided OFDM," *IEEE Access*, vol. 5, pp. 50–60, 2017.

[10] T. Mao, Q. Wang, and Z. Wang, "Generalized dual-mode index modulation aided OFDM," *IEEE Communications Letters*, vol. 21, no. 4, pp. 761–764, April 2017.

[11] K. O. Akande and W. O. Popoola, "Experimental demonstration of subband index techniques for m-CAP in short-range SI-POF links," *IEEE Photonics Technology Letters*, vol. 30, no. 24, pp. 2155–2158, Dec 2018.

[12] Q. Wang, T. Mao, and Z. Wang, "Index modulation-aided OFDM for visible light communications," in *Visible Light Communications*, J.-Y. Wang, Ed. Rijeka: InTech, 2017, ch. 4.

[13] G. Foschini, R. Gitlin, and S. Weinstein, "Optimization of two-dimensional signal constellations in the presence of Gaussian noise," *IEEE Transactions on Communications*, vol. 22, no. 1, pp. 28–38, January 1974.

[14] M. Wen *et al.*, "Multiple-mode orthogonal frequency division multiplexing with index modulation," *IEEE Transactions on Communications*, vol. 65, no. 9, pp. 3892–3906, Sept 2017.

[15] E. Baar, Ü. Aygölü, E. Panayrc, and H. V. Poor, "Orthogonal frequency division multiplexing with index modulation," in *2012 IEEE Global Communications Conference (GLOBECOM)*, Dec 2012, pp. 4741–4746.